Available online at www.sciencedirect.com
SCIENCE DIRECT
Polymer 47 (2006) 2865–2873
polymer
www.elsevier.com/locate/polymer

Nanomechanical and surface frictional characteristics of a copolymer based on benzoyl-1,4-phenylene and 1,3-phenylene

Sarah E. Morgan *, Rahul Misra, Paul Jones

School of Polymers and High Performance Materials, University of Southern Mississippi, Hattiesburg, MS 39406, USA

Received 22 November 2005; received in revised form 8 February 2006; accepted 9 February 2006
Available online 2 March 2006

Abstract

Surface mechanical and tribological properties of a copolymer based on benzoyl-1,4-phenylene and 1,3-phenylene were evaluated using nanoprobe investigation techniques and compared to the properties obtained at the macroscale. These copolymers are commonly referred to as self-reinforced polymers (SRPs) because of their intrinsic high strength and modulus without addition of a reinforcing agent. Specimens were prepared by spin casting, solvent casting, and compression molding. Surface mechanical properties and film thickness were measured by nanoindentation and scratching techniques. Friction properties were found using lateral force microscopy (LFM), and surface topography was imaged by tapping mode atomic force microscopy (AFM). Macroscale friction testing revealed a kinetic coefficient of friction of 0.08 for SRP, approaching that of Teflon. Similarly low relative friction coefficients were obtained in nanoprobe measurements. Nanoindentation of SRP, polycarbonate (PC), and polyetherimide (PEI) demonstrated superior surface hardness and modulus of SRP copolymer thin films.

Keywords: Nanotribology; Nanomechanical properties; Poly(*p*-phenylene)

1. Introduction

Poly(paraphenylene) is a rigid rod polymer that in theory should possess ultra high strength and stiffness due to the rigid nature of its backbone, consisting exclusively of phenylene linkages. However, during the polymerization reaction only 6–10 repeat units are incorporated into the polymer chain before it precipitates from solution [1]. Incorporation of a comonomer with benzoyl substituents renders the copolymer soluble and a copolymer with a high molecular weight and intrinsic viscosity can be produced (Fig. 1). The strength and stiffness of the material is retained by the rigid phenylene linkages throughout the backbone, while the side group attachment gives the polymer its solubility [2,3]. Linear copolymers of 1,4-phenylene with benzoyl-1,4-phenylene, however, remain difficult to process via traditional melt processing techniques such as injection molding. Incorporation of 1,3-phenylene comonomer yields a copolymer with improved melt processability, but somewhat reduced modulus. These copolymers are commonly referred to as self-reinforced polymers (SRPs) because of their intrinsic high strength and modulus without addition of a reinforcing agent. Compared to most linear polymers, which possess a more coil-like structure, SRPs have reduced conformational and rotational motion. This inhibits their ability to flex and produces a much stiffer material. The strength of SRPs is also directly related to the aspect ratio of the rod-like segments of the polymer molecule, with a higher aspect ratio yielding a stronger material [2]. The solubility, stiffness, and melt processability of the copolymers can be specifically tailored by adjusting the copolymer composition. The SRP used in this study is a commercially available copolymer with approximately 15 mol% 1,3-phenylene and 85 mol% benzoyl-1,4-phenylene [4].

SRPs are amorphous polymers that can be processed by both solution and melt techniques into transparent, amorphous films and plaques [5,6]. SRPs exhibit dramatically increased strength, modulus and hardness properties in comparison to traditional engineering thermoplastics, as exhibited in reported properties for commercial SRP, polyetherimide (PEI) and polycarbonate (PC) polymers of similar molecular weights (Table 1) [7–9]. Additionally, SRPs have been demonstrated to form miscible blends with polycarbonate with intermediate modulus levels, providing potential opportunity for more easily processable high strength transparent materials [4]. Their ultra high strength, hardness and strength to weight ratio make SRPs of interest for applications ranging from light weight structural

* Corresponding author. Tel.: +1 601 818 6728; fax: +1 601 266 5635.
E-mail address: sarah.morgan@usm.edu (S.E. Morgan).

0032-3861/$ - see front matter © 2006 Elsevier Ltd. All rights reserved.
doi:10.1016/j.polymer.2006.02.025

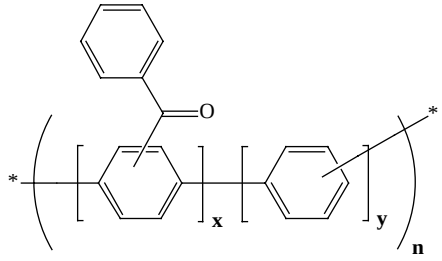

Fig. 1. Generalized chemical structure of a copolymer of benzoyl-1, 4-phenylene and 1,3-phenylene.

components to protective films and coatings. In particular, their demonstrated dielectric capabilities [6,10] combined with their high strength and hardness, indicate their potential for thin film and micro/nanoelectronic applications. For these types of applications, however, it is critical to understand not only the bulk mechanical properties, but also surface and nanomechanical performance of the materials, and property correlation from nano to macroscale. Specifically, the friction properties of SRP from nano to macroscale have been evaluated in comparison to polystyrene, which was chosen as a reference amorphous material that has been extensively characterized and whose nanotribological behavior has been previously reported [11]. Additionally, nanomechanical properties of SRP were evaluated in comparison to PEI and PC polymers, and their surface properties compared to reported bulk mechanical properties. The widely used engineering thermoplastics PEI and PC were chosen as reference comparative materials for evaluating SRP performance, and to provide materials with varying rigidity (SRP stiffness > PEI > PC). SRP, PEI and PC grades of similar molecular weights were chosen to minimize performance differences based on molecular weight.

Atomic force microscopy (AFM) and nanoindentation techniques are emerging as effective methods for measurement and prediction of thin film properties, including friction, wear, surface roughness, adhesion, lubrication, hardness, and modulus [11–14]. In this paper properties measured at both the nanoscale and macroscale are compared to assess the translation of properties from the molecular to macroscopic level, of particular interest for assessing performance for advanced thin film applications.

Amonton's law describes friction at the macroscopic level, where the frictional coefficient (μ) is the ratio of the frictional force (F_f) to the total normal force (F_n) [15,16].

$$\mu = \frac{F_f}{F_n} \tag{1}$$

However, polymeric materials deviate from this law due to effects from adhesion and surface tension [15,17]. AFM is used to evaluate relative friction measurements taking into account the adhesive forces experienced at the surface of materials under ambient conditions. The capillary forces between the tip and the liquid layer on the sample surface produce an adhesive force (F_a), which is added to the applied load (F_l) to give the total normal force applied to the sample.

$$\mu = \frac{F_f}{(F_l + F_a)} \tag{2}$$

After rearrangement the frictional force can be expressed as:

$$F_f = \mu F_l + F_a \tag{3}$$

Fiction coefficient, μ, is found from the slope of a plot of F_f as a function of F_l [18].

Indentation characterization is a valuable method for evaluating the nanoscale response of materials. These methods are used to determine local hardness and modulus on the surface of a material. Measurements are based on a force curve generated as a stiff probe penetrates the material surface. A force curve plots the applied load to the probe with respect to displacement into the specimen, and information about modulus, hardness, elastic recovery, and plastic deformation is obtained [19].

Property measurements are based on the contact mechanics of an axisymmetric indenter with an elastically isotropic half space, developed by Oliver and Pharr [20]. Hardness values (H) are calculated as:

$$H = \frac{P_{max}}{A} \tag{4}$$

P_{max}, maximum applied load; A, contact area between the probe and the specimen.

Reduced modulus (E_r) values are taken from the slope (dh/dP) of the unloading portion of the force curve and are dependant upon the contact area by the relation:

$$E_r^{-1} = \frac{dh}{dP}\frac{2A^{1/2}}{\pi^{1/2}} \tag{5}$$

h, depth of penetration; P, applied load.

Table 1
Bulk mechanical properties of SRP vs. traditional engineering thermoplastics

	SRP[a]	PEI[b]	PC[c]
Flexural modulus (MPa) ASTM D790	8300	3510	2340
Tensile stress at yield (MPa) ASTM D638	207	110	62
Rockwell hardness ASTM D785	80B (B scale)	109M (M scale)	70M (M scale)

[a] PARMAX® 1200 SRP Technical Data Sheet, http://www.mptpolymers.com.
[b] ULTEM® 1000 Technical Data Sheet, http://www.ge.com/en/.
[c] LEXAN® 144R Technical Data Sheet, http://www.ge.com/en/.

2. Experimental

2.1. Materials

Materials were used as received unless noted otherwise. Polystyrene (PS) of weight average molecular weight (M_w) 280,000 g/mol was purchased from Aldrich. SRP resin and compression molded discs were supplied by Mississippi Polymer Technologies, Inc., (MPT) Bay St Louis, MS.

The SRP copolymer evaluated, PARMAX® 1200, has M_w of 30,000 as measured by light scattering [21]. The SRP is produced on commercial scale at MPT facilities via a proprietary process [22]. PC (LEXAN® 144R) and PEI (ULTEM® 1000) molded discs were provided by GE Plastics. The PC M_w measured by light scattering (absolute method) is reported as 26,300, while the relative M_w determined by GPC using polystyrene standards is reported as 57,000 [23]. PEI relative M_w measured by GPC using polystyrene standards is reported as 52,000 [24]; actual molecular weight is in the range of 20,000–30,000 [25]. Mica discs (9.9 mm diameter, Ted Pella, Inc.) were used as the substrate for PS and SRP films.

2.2. Sample preparation

SRP and PS films were spin coated onto freshly cleaved mica substrates, using a KW-4A (CHEMAT Technology) spin coater. SRP was dissolved in benzyl chloride at two weight percent, and PS was dissolved in tetrahydrofuran (THF) at a concentration of 2 wt%. 10 μL of polymer solution was deposited on the mica disc. Spin coating was performed in two successive stages, an initial stage at 500 rpm for 15 s followed by a second stage at 3000 rpm for 45 s. Samples were dried for 3 h in ambient air followed by drying in a vacuum oven for 12 h at 70 °C.

Solution cast films of SRP and PS were prepared on glass plates using a draw down bar. SRP and PS resin were dissolved in 1-methyl-2-pyrrolidinone (NMP) and THF, respectively, at 10 wt% for solution casting.

2.3. Atomic force microscopy (AFM)

The surface topography and roughness were obtained from height images collected using the Dimension 3000 AFM (Digital Instruments, Santa Barbara, CA). The images were collected in tapping mode using an etched silicon probe, 125 μm long with a resonant frequency of 275 kHz, nominal force constant of 40 N/m and a nominal tip radius of 10 nm. Friction measurements were obtained by operating the AFM in lateral force microscopy (LFM) mode using a triangular silicon nitride probe with a nominal spring constant of 0.58 N/m.

2.3.1. Frictional force

Frictional force measurements using the AFM were carried out on spin cast films of SRP and PS. The normal applied force was calculated from force–distance curves by the product of normal deflection of the cantilever (d) and spring constant (k) of the cantilever. Deflection of the cantilever is due to intermolecular forces between the tip and surface, which may be attractive and/or repulsive in nature [18,26]. In LFM, friction force is experienced in the direction opposite to the scan direction, while the normal force acts in the direction perpendicular to both the scan direction and the friction force direction. The cantilever experiences a torque imposed by the tip, which is recorded as a voltage signal. Voltage (mV) signal is then converted to friction force (nN) based on a calibration constant from a silicon wafer, which was determined to be

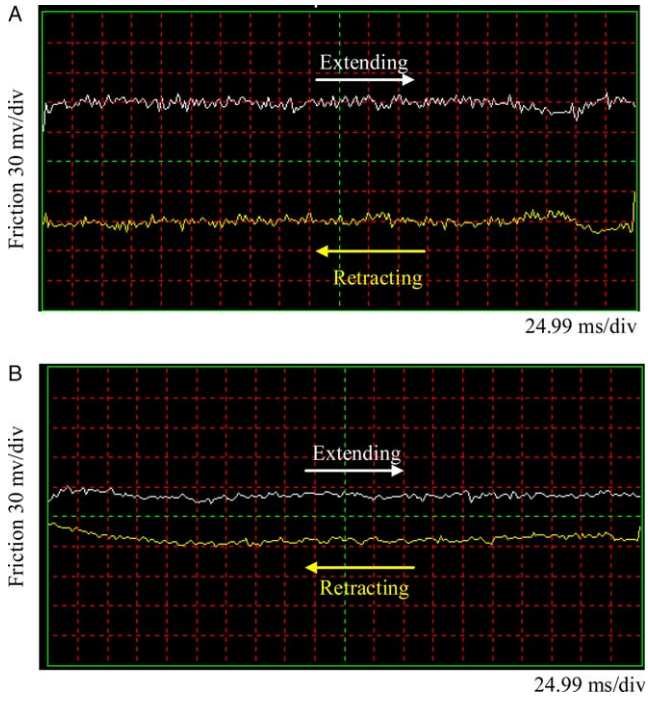

Fig. 2. Real time friction loops for (A) spin coated PS (B) spin coated SRP.

0.144 nN/mV using a reported friction coefficient of 0.06 [18]. Trace and retrace images (Fig. 2) are obtained in LFM while the tip moves over the stationary sample at a scan direction of 90°. The frictional force for a given normal load is calculated as the mean value of the separation distance between the trace and retraces signals [18,27,28].

2.3.2. Indentation and scratching

Indentation and scratch measurements were made using a MultiMode AFM (Digital Instruments, Santa Barbara, CA) and a Triboindenter (Hysitron, Inc., Minneapolis, MN). The probe used with the MultiMode was a steel cantilever mounted with a diamond tip, having a force constant of 162 N/m and resonant frequency 63.8 kHz. Deflection sensitivity of the cantilever was calibrated on a sapphire surface. The Triboindenter was operated with a three-sided diamond (Berkovich type) tip, which was calibrated on fused silica [20].

The thickness of the spin cast SRP and PS films was measured by nanoscratching and indentation. Film thickness by scratching was performed on the AFM by finding the force that produced no scratch on mica. The polymer film was then scratched at the same force until the film was removed. The furrow was then imaged to obtain film thickness. Film thickness from indentation was measured using the Triboindenter. The load was applied to the surface at linear loading and unloading rate of 10 μN/s with 2 s hold period at the maximum applied load. Nanoindentation was performed under closed loop with load control using compliance method in which force–displacements curves are obtained during loading and unloading cycles. As the indenter presses into the surface the displacement is recorded as a function of the applied load.

Nanoindentation using a MultiMode AFM was performed on solvent cast SRP films and extruded PC films. Deflection

sensitivity of the cantilever was determined from indenting an impenetrable sapphire surface. A 4×4 array of indents spaced by 750 nm with the applied load increasing by equal increments of 3.4 μN from 13.7 to 23.9 μN along each row was made into PC and SRP surfaces. Immediately after indentation the arrays were imaged.

Nanoindentation of SRP, PC, and PEI compression molded discs was performed using a Triboindenter mounted with a Berkovich tip. A single indentation sequence was used for all three specimens. The applied force was linearly ramped from 0 to 8 mN over a period of 10 s with a 16s hold time at the maximum force and removed linearly over a period of 10 s.

2.4. Macroscale friction evaluation

Dynamic friction coefficient measurements were performed according to ASTM D1894-01, [29] using a Dynisco D1055 coefficient of friction tester (Dynisco Polymer Test, MA). Three sets of readings were taken for each sample ($5'' \times 10''$) under atmospheric conditions and then averaged to obtain relative kinetic coefficient of friction (COF). Samples were measured at a sliding velocity of 0.25 cm/s and 20 °C.

2.5. Water contact angle

Water contact angle measurements were conducted using sessile drop technique by a First Ten Angstroms (FTA, Portsmouth, VA) contact angle goniometer coupled with FTA 200 data analysis software.

3. Results and discussion

3.1. Friction analysis

Macroscale friction evaluations were performed on bulk solvent-cast PS and SRP films for comparative purposes with nanotribological evaluations. SRP demonstrates dramatically reduced kinetic coefficient of friction (COF) in comparison to PS, with measured values of 0.08 for SRP and 0.34 for PS (Table 2). In fact, the measured COF for the SRP film approaches that of Teflon, reported as 0.04 [30]. Note that the measured kinetic COF for polystyrene is consistent with commonly reported values [31,32]. Typical amorphous plastics exhibit COF values similar to or higher than that of PS [33]. The ultra low friction behavior of SRPs is attributed to their regular molecular profile as well as to their outstanding mechanical properties (Table 1), which distinguish SRPs from classical amorphous polymers. In their pioneering work on

Table 2
AFM roughness analysis of spin coated polymer samples

Sample	Max height (nm)	Mean roughness (nm)	RMS roughness (nm)
Freshly cleaved mica	1.35	0.11	0.15
PS on mica	2.61	0.21	0.26
SRP on mica	10.01	0.23	0.30

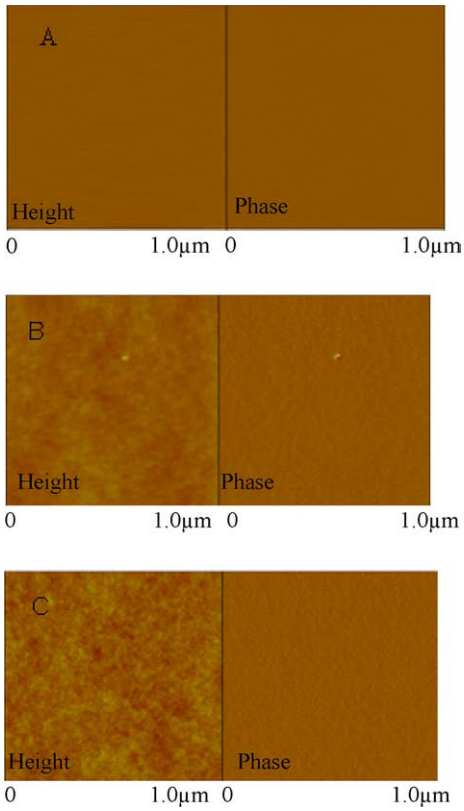

Fig. 3. Height and phase image of (A) freshly cleaved mica (B) polystyrene (PS) (C) self reinforced polymer (SRP).

friction and molecular structure, Pooley and Tabor [33] demonstrate that during the sliding process the strength of adhesion at the interface and the bulk shear strength of the sliding bodies can be linked to the frictional characteristics of

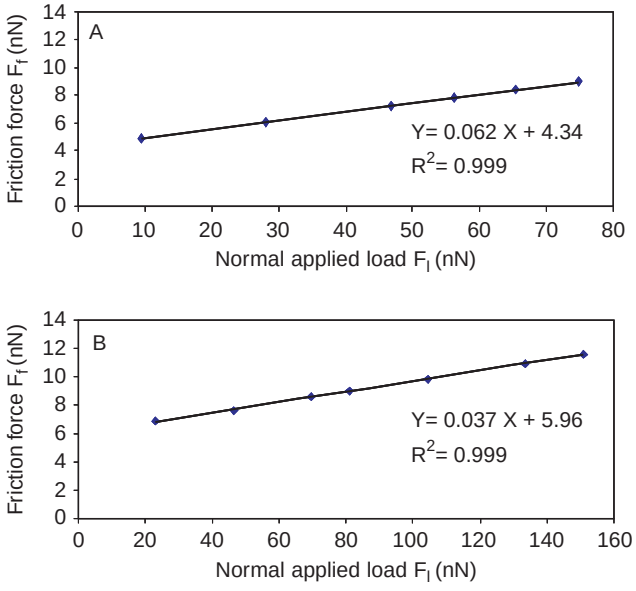

Fig. 4. Friction force vs. normal force plot for spin coated (A) neat PS (B) neat SRP onto mica.

Table 3
Macro and nanoscale friction coefficients

Sample	Macro kinetic COF	Nano relative COF
PS on mica	0.34	0.062
SRP on mica	0.08	0.037

Table 4
Adhesive force and water contact angle for PS and SRP films

Sample	Adhesive force (nN) from force curve	Adhesive force (nN) from friction plot	Water contact angle (°)
PS on mica	61	70	88
SRP on mica	120	160	82

the surfaces in contact. Relatively greater shearing will be observed in the bulk of the polymer if the interfacial shear strength is greater than the bulk shear strength, whereas higher bulk strength compared to interfacial shear strength will facilitate shearing at the interface. Bulk transfer of material generally leads to higher friction [33,34]. In semi-crystalline polymers, reduced friction may result from orientation of crystalline chains in the direction of shear. In the case of teflon, the extremely low friction is attributed to the formation of a transfer film combined with orientation of crystalline chains in the sliding direction [33,34]. In amorphous polymers, where little orientation is expected, the friction is related to hardness of the surface and the ability to resist formation of wear particles that can increase friction. Due to their high surface hardness and modulus, SRPs exhibit greater resistance to plastic deformation, scratching, and wear than typical thermoplastics. Although SRPs are amorphous and transparent, some level of shear-induced orientation may occur at the surface that facilitates sliding because of their highly linear structure and stiff main chain. These factors combined provide an explanation for the very low friction coefficient observed for SRP in macroscale testing.

Similar trends are observed in nano-friction evaluations. Freshly cleaved mica was selected as the substrate for preparation of spin coated polymer films to avoid external contamination and to ensure a nanoscopically smooth substrate for film deposition. Spin casting yielded smooth, transparent films of SRP and PS. Comparative AFM height and phase images indicate coverage of the cleaved mica surface with the polymer films (Fig. 3), with a slight increase in roughness exhibited for the film-coated surfaces (Table 2). The films remain exceptionally smooth, however, with a root mean square (RMS) roughness of less than 0.3 nm for both SRP and PS. This low level of surface roughness is desired for accurate nano-friction measurements.

Representative lateral friction loops are shown in Fig. 2. At equivalent applied loads, SRP films demonstrated lower friction than PS films, reflected by the smaller distance between the trace and retrace curves for SRP. This is seen more clearly in plots of friction force as a function of applied

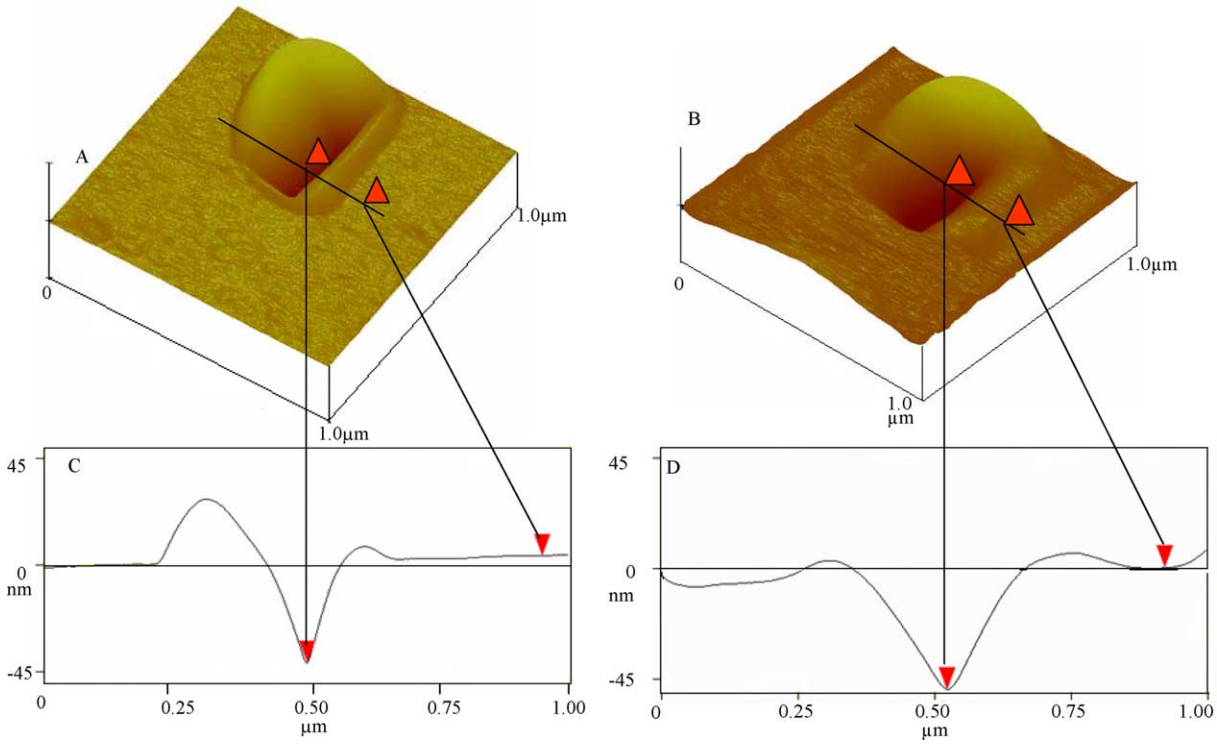

Fig. 5. Scratch image of (A) neat SRP (B) neat PS, section analysis of scratched (C) neat SRP (D) neat PS.

load (Fig. 4). Both systems yield linear relationships. Relative coefficient of friction is obtained from slope of the lines, with SRP films providing relative friction coefficient approximately half that of PS films (Table 3). In fact, the low COF of 0.037 measured for SRP approaches that of Teflon nanotribology evaluations, with reported COF of approximately 0.03 [35]. These very low nanoscale friction coefficients indicate the potential utility of SRP materials for thin film low friction applications.

Although the absolute values of the measured COF's differ for macro and nanoscale testing, with significantly lower values measured via AFM, the relative trends for the materials are the same as evaluated via both methods. Comparatively low values for AFM friction measurements are commonly reported [18], and the measured COF of 0.06 for polystyrene is in the range of nanoprobe measurements reported by other researchers [11]. It has been suggested that these differences in magnitude are related to effects of adhesion forces at the nanoscale and/or differences in surface damage at macro vs. nanoscale [36,37]. The relative friction coefficient depends on the true area of contact between the surfaces. In macroscale friction testing, the area of contact as well as the surface asperities in contact between the sliding surfaces are orders of magnitude higher than at the nanoscale. Thus, a substantially higher number of wear particles are produced, causing greater bulk deformation and plowing of the polymer surface, resulting in a substantially higher measured COF at macroscale. Additionally, increased shear force is required due to the greater number of asperities at the surface, contributing to the higher COF at macroscale.

The adhesive force (F_a) between the AFM tip and the substrate was estimated from force curves and from the intercept of the friction force vs. applied load plots (Table 4). Good agreement is obtained for F_a values estimated by the two methods. Although all F_a values are of similar magnitude, a somewhat greater adhesive force is observed between the probe and the SRP film than to the PS film, possibly due to interaction between hydrophilic substituents on the SRP polymer chain and the hydrophilic silicon nitride probe. Water contact angle measurements (Table 4) do not indicate large differences in hydrophilicity of the films, although the SRP films demonstrated slightly lower contact angle in comparison to PS (82 and 88°, respectively). Lower adhesive forces demonstrated for PS and the probe tip can explain differences in the relative COF values at macro and nanoscale. In macroscale friction testing, the SRP friction coefficient is one-fourth that of PS, while in nanoscale friction testing the SRP friction coefficient is approximately one-half that of PS. The relative differences can also be explained by differences in orientation of the films due to film preparation method (spin coating vs. draw-down bar). It was not possible to perform macroscale friction testing on the spin coated samples due to the small dimensions of the films.

3.2. Film thickness

Film thickness was estimated by AFM using a nanoscratching method and by the Triboindenter using indentation

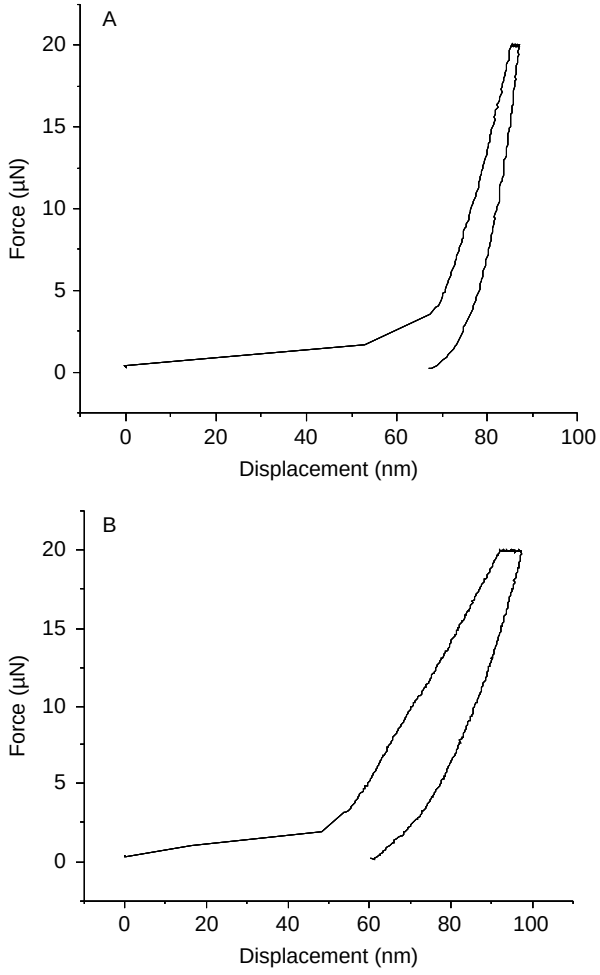

Fig. 6. Hysitron nanoindentation force vs. displacement plot for (A) SRP (B) PS onto Mica

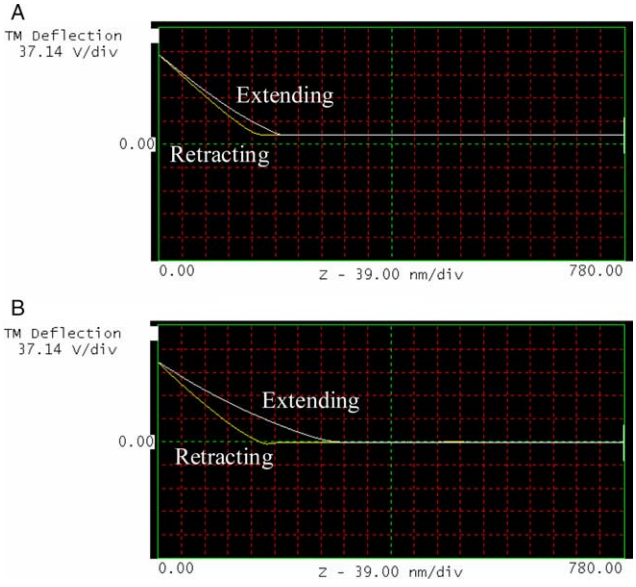

Fig. 7. Force curves for (A) SRP and (B) PC indentation

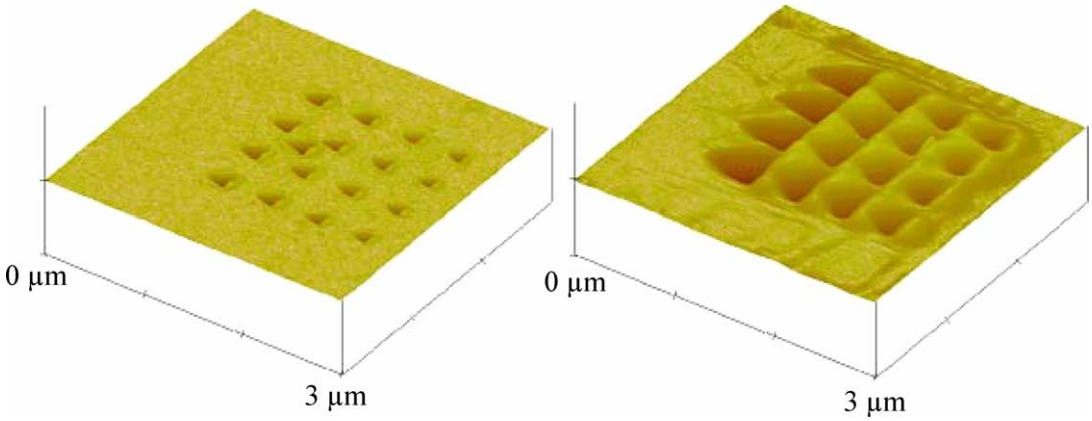

Fig. 8. Tapping mode images for (A) SRP and (B) PC indent arrays. Height scale is set to 150 nm.

methods. Results show good agreement between the two methods. The AFM nanoindentation method has greater sensitivity and provides higher levels of resolution for force–distance measurements, however, the method utilizing the Hysitron Triboindenter is faster and yields simpler data analysis. As seen in Fig. 5, AFM section analysis of nanoscratched film surface indicates film thickness of spin coated SRP and PS to be approximately 45 and 50 nm. Film thickness is determined by taking the average difference in height of the film surface away from the furrow and at the substrate where the film was removed, taking care to avoid the area of built-up material caused by displacement of material during the scratching process (Fig. 5). Using the Triboindenter, thickness, which is indicated by the change in slope in the force–distance curve (Fig. 6), is estimated to be approximately 48 and 52 nm for PS and SRP samples, respectively. Film thicknesses measured by the two techniques agreed within 5 nm.

3.3. Nanoindentation of polymer films and compression molded specimens

Nanoindentation studies were performed on SRP samples to determine comparative hardness and elasticity of thin films and surfaces at nanoscale in relation to bulk measurements. SRP and PC films were analyzed via AFM nanoindentation techniques, as described in the experimental section. In this study, an indent array was created using increasing levels of force on the film surface. The same array was applied to both SRP and PC, and as observed in Figs. 7 and 8, indentation depth and deformation of the surface is substantially greater for the PC film. The maximum indentation depth is extracted from the force curve obtained during the indentation process. The maximum occurs when the tip is at the highest deflection and maximum z-piezo travel (Fig. 7). Maximum indentation depths for each level of applied force are given in Table 5. For the lowest levels of applied force indentation depth is two times greater for PC than SRP, increasing to 3:1 indentation depths for PC compared to SRP at higher levels of force. Residual indentation depth is determined by imaging the films in tapping mode after completing the indentation array (Fig. 8). As seen for maximum penetration depth, PC exhibits two to three times greater residual indentation depth than SRP, with the difference in indentation levels increasing with increasing applied load (Table 5). Percent recovery is defined as the difference in maximum penetration depth and residual indentation depth divided by the maximum indent depth. Average recovery for both materials is 70–75%. Thus, although plastic deformation is substantially higher for the PC film, elastic recovery is similar for the two amorphous polymers.

Nanomechanical analysis of compression molded SRP, PEI and PC samples was performed using the Hysitron Triboindenter to determine surface hardness and reduced modulus via the methods described in the Sections 1 and 2. As seen in Fig. 9, penetration of the diamond tip as well as deformation (as indicated by final depth at pull-off load = zero on retraction curve) are dramatically greater for both PEI and PC in comparison to SRP. As was observed in AFM measurements, penetration depth is three to four times higher for PC than for SRP for the same loading force. Plastic deformation is approximately two times greater for PEI and three times greater for PC than for SRP. Reduced modulus and hardness data for the molded samples are summarized in Table 6. Reduced modulus measured via the nanoindentation method exhibits the same trends observed in bulk testing (Table 1), with SRP demonstrating a reduced modulus that is more than twice that of PEI and almost three times that of PC. Similarly, nanoscale hardness evaluations display the trends observed in

Table 5
Maximum indentation depth, residual indentation depth, and percent recovery of SRP and PC. Each value is an average of the values from four indents

Sample	Force (μN)	Max indent depth (nm)	Residual indent depth (nm)	% Recovery
SRP	13.7	63	15	76
	17.1	68	18	74
	20.5	62	21	64
	23.9	81	23	72
PC	13.7	140	26	82
	17.1	156	40	78
	20.5	180	42	76
	23.9	190	64	66

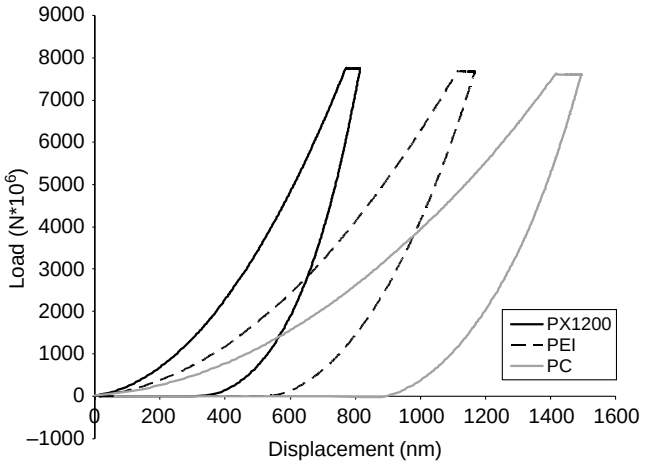

Fig. 9. Force curves for SRP, PEI, and PC compression molded samples from Triboindenter.

macroscale Rockwell hardness tests, with substantially greater hardness for the SRP molded sample. The observed nano and macroscale properties follow expected trends, with hardness and modulus increasing with increasing chain stiffness. SRP exhibits highest modulus and strength due to the high proportion of paraphenylene linkages and restricted rotational movement along the main chain [38], followed by PEI [39,40] and finally PC [41].Thus the incorporation of metaphenylene linkages in the SRP copolymer, at least at the copolymer level tested, provides improved processability while maintaining high surface hardness and modulus for SRP in comparison to traditional engineering thermoplastics. These findings indicate the potential utility of SRPs for thin film applications requiring high strength and modulus. Nanoindentation results also provide some insight into the mechanism for the improved friction properties of SRPs, as friction behavior depends on mechanical properties in addition to the chemical nature of the polymer and the adhesion between the surfaces in contact. The ultra high hardness and modulus exhibited by SRPs in nanoindentation evaluations indicate their greater resistance to plastic deformation, scratching, and wear as well as resistance to local penetration on application of external force. These combined mechanical properties factor in the observed low friction coefficients for SRP films at macro and nanoscale. Observed low coefficients of friction also indicate the absence of significant effects of asperities and wear particles, and that interfacial adhesion in the employed test conditions is not strong compared to the bulk cohesion. The low friction behavior of SRPs can be attributed to their regular semi-rigid rod molecular profile combined with their superior mechanical properties.

Table 6
Reduced modulus and hardness for SRP, PEI and PC molded samples obtained via Hysitron Triboindenter nanoindentation

Sample	Reduced modulus (GPa)	Hardness (MPa)
SRP	10.23	688
PEI	4.55	357
PC	3.57	188

4. Conclusions

Copolymers based on benzoyl-1,4-poly(*p*-phenylene) and 1,3-phenylene are readily processed via solution and melt processing techniques. Spin coating from benzyl chloride solution yields transparent, thin (~50 nm) smooth films, with measured RMS surface roughness of 0.3 nm. These materials show very low friction, whether measured at nano or macroscale, with measured kinetic coefficient of friction (0.08) in macro testing approaching that of Teflon. Relative friction coefficients measured via LFM show similar trends, although the values of COF are substantially lower when measured using nanoprobe techniques. Low values of friction coefficients for SRPs at macro and nanoscales indicate their higher wear resistance and better lubrication properties at both scales which are highly desired for potential biomedical and electronic devices applications. In macroscale testing, the ratio of PS to SRP COF is four to one, while in LFM testing PS to SRP COF ratio is two to one. This may be explained in part by the relatively higher attractive force between the AFM tip and the SRP film in comparison to the PS film. In nanoindentation studies, SRP molded samples demonstrated one and a half to two times the surface hardness and reduced modulus of traditional engineering thermoplastics. These improved nanomechanical properties also contribute towards low friction coefficients of SRPs at nanoscale by providing more resistance to wear, deformation and local penetration. The extremely low coefficient of friction combined with high modulus and surface hardness of these thin films indicate their potential utility for advanced thin film applications.

Acknowledgements

Acknowledgement is made to the donors of the American Chemical Society Petroleum Research Fund for support of this research. Additionally, this work was partially supported by the MRSEC Program of the National Science Foundation under Award Number DMR 0213883 and MRI Award Number 0421403. Acknowledgements are also due to Mississippi Polymer Technologies, Inc, (Bay St Louis, MS) and GE Plastics for providing the polymer samples, and Dr Sergei Magonov (VEECO Industries, CA) for valuable discussions and inputs during this study.

References

[1] Odian G. Principles of polymerization. 3rd ed. New York: Wiley; 1991. p. 175.
[2] Marrocco III ML, Gagné RR, Trimmer MS. US Patent 5,227,457; issued July 13, 1993.
[3] Wang GY, Quirk RP. Macromolecules 1995;28(10):3495–501.
[4] Ha YH, Scott CE, Thomas EL. Polymer 2001;42:6463–72.
[5] Hwang WF, Helminiak TE. Mater Res Soc Symp Proc 1989;134:507–9.
[6] Connolly M, Karasz F, Trimmer M. Macromolecules 1995;28:1872–81.
[7] PARMAX® 1200 SRP Technical Data Sheet http://www.mptpolymers.com, accessed 1/06.
[8] ULTEM® 1000 Technical Data Sheet http://www.ge.com/en/, accessed 1/06.
[9] LEXAN® 144R Technical Data Sheet http://www.ge.com/en/, accessed 1/06.

[10] Jones PJ, Malkovich N, Thomas DB, Morgan SE. Annual technical conference—society of plastics engineers. 63rd ed; 2005. p. 2067–69.
[11] Chen YW, Gan DJ, Kreiling S, Song CS, Lu SQ, Wang Z. J Appl Phys A 2003;76:129–32.
[12] Bhushan B. Wear 2001;251:1105–23.
[13] Li J, Wang C, Shang G, Xu Q, Zhand L, Guan J, Bai C. Langmuir 1999; 15:7662–9.
[14] Michel D, Kopp-Marsaudon K, Aime J. Tribol Lett 1998;4:75–80.
[15] Howell HG, Mazur JJ. Text Inst 1953;44:T59–T69.
[16] Adamson AW. Physical chemistry. New York: Wiley; 1990. p. 460–89.
[17] Bowden FP, Taber D. Friction and lubrication. London: Oxford University Press; 1956.
[18] Ruan JA, Bhushan B. J Tribol 1994;116:378.
[19] VanLandingham MR, McKnight SH, Palmese GR, Elings JR, Huang X, Bogetti TA, et al. J Adhes 1997;64:31–59.
[20] Oliver WC, Pharr GM. J Mater Res 1992;7:1564–83.
[21] Communicated by MPT.
[22] Marrocco III ML, Gagne RR, Trimmer MS. US Patent 5,227,457. Assigned Maxdem, Inc.; 1989.
[23] Brunelle DJ, Kailasam G. Polycarbonates, GE Global Research Technical Reports, http://www.crd.ge.com/cooltechnologies/biblio/2001crd136_bib.jsp (accessed October 2004); 1989.
[24] Sanner MA, Haralur G, May A. J Appl Polym Sci 2004;92:1666–71.
[25] Alfageme JA, Iriarte M, Iruin JJ, Etxeberria A, Uriarte C. Appl Polym Sci 1999;73(3):323–32.
[26] Magonov SN. In: Meyers RAd, editor. Encyclopedia of analytical chemistry. Chichester: Wiley; 2000.
[27] Clark HA, Plueddeman EP. Mod Plast 1963;40:133–5.
[28] Baselt DR, Baldeshwielder JD. J Vac Sci Technol B 1992;10:2316–22.
[29] ASTM D 1894-01; standard test method for static and kinetic coefficients of friction of plastic film and sheeting.
[30] Walker JS. Physics. 2nd ed. New Jersey: Pearson Education; 2004. p. 139.
[31] McLaren KG, Tabor D. Nature 1963;197:856.
[32] Rudd JF. Handb Polym 1998;5:81.
[33] Pooley CM, Tabor D. Proc R Soc, London A 1972;329:251–74.
[34] Biswas SK, Vijayan K. Wear 1992;158:193–211.
[35] Podesta A, Fantoni G, Milani P, Guida C, Volponi S. Thin Solid Films 2002;419:154–9.
[36] Koinkar VN, Bhushan B. J Vac Sci Technol 1996;A14(4):2378.
[37] McClelland GM. Adhesion and friction. Berlin: Springer; 1989. p. 1.
[38] Vaia RA, Dudis D, Henes J. Polymer 1998;39:6021–36.
[39] Davies M, Hay JN, Woodfine B. High Perform Polym 1993;5(1): 37–45.
[40] Takekoshi T, Kochanowski JE, Manello JS, Webber MJ. Polym Prepr 1983;24(2):312–3.
[41] Li X, Yee AF. Macromolecules 2004;37(19):7231–329.